JOURNAL OF MATERIALS SCIENCE 26 (1991) 6401–6407

Growth of emerald crystals from $PbO \cdot V_2O_5$ flux

SHUJI OISHI, MINORU HIRAO
Department of Chemistry and Material Engineering, Faculty of Engineering, Shinshu University, Wakasato, Nagano 380, Japan

The flux growth of emerald crystals by slow cooling in the $PbO \cdot V_2O_5$ flux is reported. The crystals exhibited the typical emerald-green colour, were up to 1.8 mm in size and transparent. Their form was a regular hexagonal rod bounded by the well-developed $\{0001\}$ and $\{10\bar{1}0\}$ faces. The solubility of emerald in $PbO \cdot V_2O_5$ was also investigated; about 9.0 g emerald was dissolved in 100 g $PbO \cdot V_2O_5$ at 1200 °C. The solubility decreased gradually with decreasing temperature. Taking the solubility data into account, the presence of undissolved particles in the solution was found to be a necessary condition for the growth of large emerald crystals. Unsaturated solution at a soak temperature produced good and relatively small emerald crystals in a subsequent cooling experiment. Advantages of the $PbO \cdot V_2O_5$ flux are also mentioned. Emerald crystals showing various kinds of imperfections, and even good crystals, were also present.

1. Introduction

Emerald ($Be_3Al_2Si_6O_{18}$:Cr) is a beryl (beryllium aluminium silicate) doped with chromium and the most attractive green gemstone. The green colour is due to the presence of a little chromium. Synthetic emerald crystals have always been of considerable interest for gemstones and other applications. The first successful synthesis of emerald crystals was reported by Hautefeuille and Perrey in 1888 [1, 2]. They grew emerald crystals from $Li_2Mo_2O_7$ and $LiVO_3$ fluxes [1, 2]. Because emerald melts incongruently [3], the crystals have been mainly grown by the flux and hydrothermal methods [2, 4]. There have been a number of investigations into the flux growth of emerald crystals. It has been found that the following fluxes can be used successfully [2, 4]; B_2O_3, V_2O_5, Li_2O–V_2O_5, PbO–V_2O_5, Li_2O–MoO_3, PbO–MoO_3, Li_2O–WO_3, PbO–WO_3 and Na_2O–B_2O_3–SiO_2.

Wanklyn [5] and Garton *et al.* [6] found that PbO–V_2O_5 flux is particularly suitable for the crystal growth of a number of simple and complex oxides. The PbO–V_2O_5 system has a eutectic at around 470 °C, 50 mol% V_2O_5 [7]. Linares [8] has grown emerald crystals from PbO–V_2O_5 flux containing between 50 and 66 mol% V_2O_5 using slow-cooling and gradient techniques. No work has been reported on the fundamental data of the solubility of emerald in molten PbO–V_2O_5.

The present paper describes the growth of emerald crystals from $PbO \cdot V_2O_5$ flux by a slow cooling method. The $PbO \cdot V_2O_5$ flux was chosen because many preliminary experiments showed it to be promising. The solubility of emerald in $PbO \cdot V_2O_5$ was also determined. Taking the solubility data into account, the effect of the soak temperature or composition of mixtures on the flux growth of emerald crystals was investigated. The crystals obtained were examined by an X-ray diffraction method, and observed by optical microscopy. In addition, the advantages of the $PbO \cdot V_2O_5$ flux for the growth of emerald crystals are discussed. It was also confirmed that the PbO–V_2O_5 system proposed as a flux for the growth of many materials [5, 6] was suitable for the growth of emerald crystals.

2. Experimental procedure

2.1. Flux growth

Stoichiometric amounts of reagent grade BeO, Al_2O_3 and SiO_2 were mixed. The oxide dopant (Cr_2O_3) was added as 1 wt % of the beryl mixture. The mixture was used as a solute for flux growth runs. An equimolar mixture (32.41 g) of reagent grade PbO and V_2O_5 was used as a flux.

The starting compositions are given in Table I. In Runs 1–5, the solute:flux ratio was unchanged and determined by reference to the data obtained by Linares [7]. In Runs 6 and 7, the solute:flux ratios were determined on the basis of the solubility data obtained in this study. The solute and flux powders were weighed out, mixed together and put into 30 cm^3 capacity platinum crucibles. The lids were tightly fitted and the crucibles were placed in an electric furnace with silicon carbide heating elements. The furnace was heated at a rate of about 50 °C h^{-1} to 900, 1000, 1100, 1150 or 1200 °C, held at this temperature for 10 h and then cooled at a rate of 5 °C h^{-1} to 600 °C. When the cooling programme was completed the furnace was allowed to cool to room temperature. Crystal products were separated by dissolving the flux in hot dilute nitric acid. The crystals obtained were investigated by X-ray diffraction (XRD) and observed using the optical microscopy.

2.2. Solubility

The solubility of emerald in an equimolar mixture of PbO and V_2O_5 was determined by measuring the

0022–2461/91 $03.00 + .12

TABLE I Starting composition, soak temperature and crystal products

Run	Composition (g)			Soak temp. (°C)	Crystal product
	Solute	PbO	V_2O_5		
1	8.00	17.86	14.55	900	No crystals grew
2	8.00	17.86	14.55	1000	Greenish hexagonal rods up to 1.0 mm × 0.5 mm × 0.5 mm in size
3	8.00	17.86	14.55	1100	Greenish hexagonal rods up to 1.2 mm × 0.8 mm × 0.8 mm in size
4	8.00	17.86	14.55	1150	Greenish hexagonal rods up to 1.5 mm × 1.0 mm × 1.0 mm in size
5	8.00	17.86	14.55	1200	Greenish hexagonal rods up to 1.8 mm × 1.2 mm × 1.2 mm in size
6	2.78	17.86	14.55	1200	Greenish hexagonal rods up to 1.2 mm × 0.8 mm × 0.8 mm in size
7	2.64	17.86	14.55	1200	Greenish hexagonal rods up to 1.2 mm × 0.8 mm × 0.8 mm in size

weight loss of emerald crystals in the $PbO \cdot V_2O_5$ melt at temperatures between 800 and 1200 °C. Mixtures of excess crystals (1–1.5 mm in size) of emerald and $PbO \cdot V_2O_5$ powder were put into platinum vessels. The total charge was 2–3 g. After dissolution had proceeded for 10 h at a controlled temperature, undissolved crystals were present on quenching. The undissolved crystals were separated from the solidified saturated solution in hot dilute nitric acid and reweighed. The loss in weight due to dissolution represents the solubility at that temperature.

3. Results and discussion

3.1. Solubility of emerald in $PbO \cdot V_2O_5$

The solubility of emerald in $PbO \cdot V_2O_5$ was determined within the range 800–1200 °C. It was confirmed in preliminary experiments that maintaining a given temperature for 10 h was sufficient time for equilibration. Evaporation of $PbO \cdot V_2O_5$ was scarcely observed during solubility experiments.

The dependence of solubility on temperature is shown in Fig. 1. At 800 °C, emerald was dissolved in 100 g $PbO \cdot V_2O_5$ at a concentration of about 0.8 g. The solubility increased gradually with increasing temperature. At 1200 °C, emerald had a solubility of about 9.0 g. The solubility curve had an appreciable temperature coefficient of solubility. It was, therefore, considered that emerald could be crystallized by slowly cooling the solutions.

Ushio and Sumiyoshi [9] have reported that about 10.7 g emerald was dissolved in 100 g V_2O_5 at 1100 °C. At the same temperature, 100 g $PbO \cdot V_2O_5$ dissolved emerald at a concentration of about 4.9 g on the basis of the solubility data obtained in this study. The solubility of emerald in $PbO \cdot V_2O_5$ is lower than that in V_2O_5: the addition of PbO to V_2O_5 reduces the degree of solubility.

3.2. Flux growth of emerald crystals

As shown in Table I, emerald crystals grew in Runs 2–7. Hexagonal rod crystals, up to 1.8 mm in size and green, were grown. The crystals were transparent. Typical crystals grown are shown in Fig. 2. The crystals obtained were identified from their XRD patterns, using data given in the JCPDS card [10]. The form and colour of the emerald crystals were not related to the growth conditions.

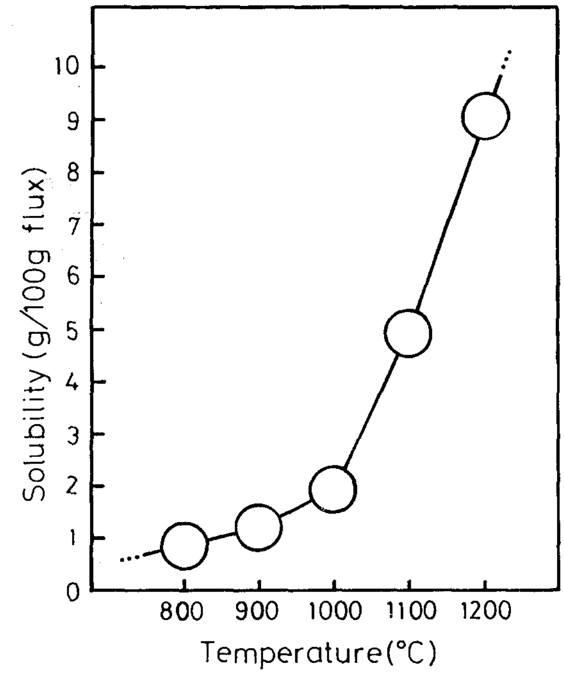

Figure 1 Solubility of emerald in $PbO \cdot V_2O_5$ as a function of temperature.

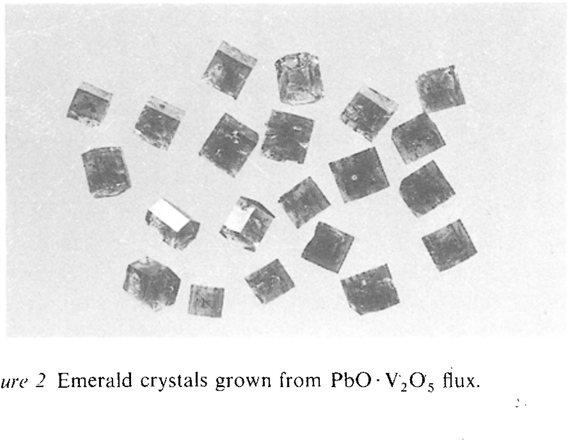

Figure 2 Emerald crystals grown from $PbO \cdot V_2O_5$ flux.

The effect of the soak temperature on the growth of emerald crystals from the high-temperature solution in a given starting composition was investigated in Runs 1–5. The composition of the mixtures used corresponds to solute (24.68 g)–flux (100 g). No crystal products were obtained in Run 1; emerald crystals were grown in Runs 2–5. Fig. 3 shows the weights of the first ten largest crystals selected plotted against

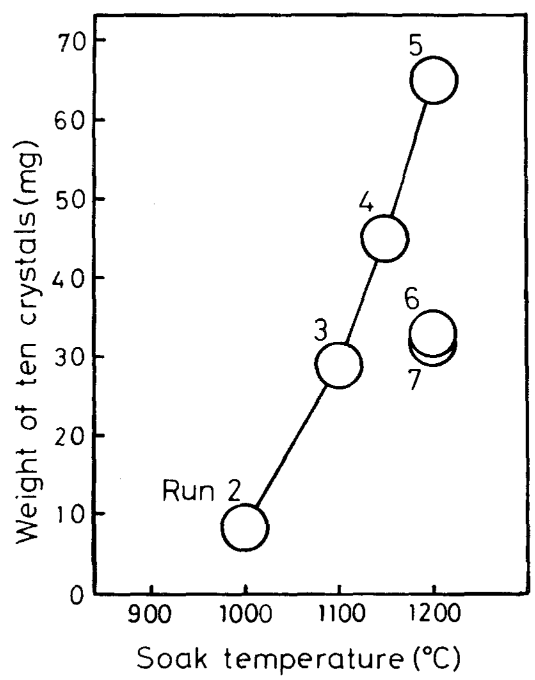

Figure 3 Variation in the weight of the first ten largest crystals selected, with soak temperature.

soak temperature. When the soak temperature was 1200 °C, the weight of the ten crystals grown was about 65 mg. The crystal weight decreased with decreasing soak temperature, until at a soak temperature of 1000 °C, the weight of the ten crystals grown was only about 8 mg. The weights of the crystals grown were evidently dependent on the soak temperatures. This tendency is attributed to the solute solubility at the respective soak temperatures. On the basis of the solubility data shown in Fig. 1, the solute is present in a large excess (about 5.1 g) in the starting mixture even at a soak temperature of 1200 °C. Therefore, considerable undissolved solute particles were present in the solutions in Runs 1–5. Any undissolved solute particles in the high-temperature solutions were likely to act as nucleation centres when crystallization occurred.

In the case of Runs 6 and 7, crystals were grown from unsaturated solutions at the soak temperature of 1200 °C in a subsequent slow cooling experiment. The solute contents of Runs 6 and 7 correspond to the amounts of 95 and 90 wt % emerald solubility at 1200 °C, respectively. The mixtures used for Runs 6 and 7 produced transparent green crystals up to 1.2 mm in size. As shown in Fig. 3, the first ten largest crystals selected grown in Runs 6 and 7 were about 33 and 32 mg in weight, respectively. Crystals grown in Runs 6 and 7 were smaller than those grown in Run 5. In Run 5, as described above, it seems that any undissolved solute particles acted as nuclei on which larger crystals grew. The presence of undissolved particles is considered to be a necessary condition for the growth of large emerald crystals. Remeika [11] has reported that $BaTiO_3$ butterfly-twins grew from KF flux. In the flux growth of the twins, DeVries and Sears [12] have described that the persistence of undissolved particles is a necessary condition for large platy growth. Generally speaking, however, the number of crystals grown from high-temperature solutions decreases with increasing difference (ΔT_{SL}) between the soak (T_S) and liquidus (T_L) temperatures, $\Delta T_{SL} = T_S - T_L$. It has been found that a small number of large crystals was obtained when the soak temperature was well above the liquidus temperature [13, 14]. For example, about 36 g solution of $CaWO_4$–Na_2WO_4 with $\Delta T_{SL} = 340$ °C produced 226 crystals of $CaWO_4$ measuring about 2.2 mm on average [14]. When ΔT_{SL} was − 70 °C, $CaWO_4$ crystals (about 0.9 mm average size) amounting to 1788 were grown [14].

The flux of $PbO \cdot V_2O_5$ produced emerald crystals as the only crystal product. One of the principal advantages of the $PbO \cdot V_2O_5$ flux is that emerald is the only stable solid phase at growth conditions. For example, Li_2O–MoO_3 and Li_2O–V_2O_5 fluxes produced unwanted crystal phases such as SiO_2, Be_2SiO_4 $BeAl_2O_4$ and $LiAlSi_2O_6$ [15–18].

A schematic drawing to show the mode of occurrence of emerald crystals in high-temperature solution is given in Fig. 4. The emerald crystals were grown at the surface of the high-temperature solution and into the upper half of the solution. Hexagonal rod crystals of emerald grew in various directions. Emerald crystals (2.64 g cm^{-3}) [10] are much less dense than $PbO \cdot V_2O_5$ flux. As any solute particles remain undissolved in Runs 2–5, the particles float and may act as nucleation centres. In Runs 6 and 7, emerald nucleates and grows in the upper parts of the solution. The position of nucleation and growth sites was remarkably related to the relative densities of crystal and flux. Emerald crystals generally grew at well-separated sites. On the other hand, a few aggregates of emerald crystals, as shown in Fig. 5, were grown in the respective growth runs.

Fig. 6 shows the evaporation losses of flux in the respective growth runs. Evaporation losses in the

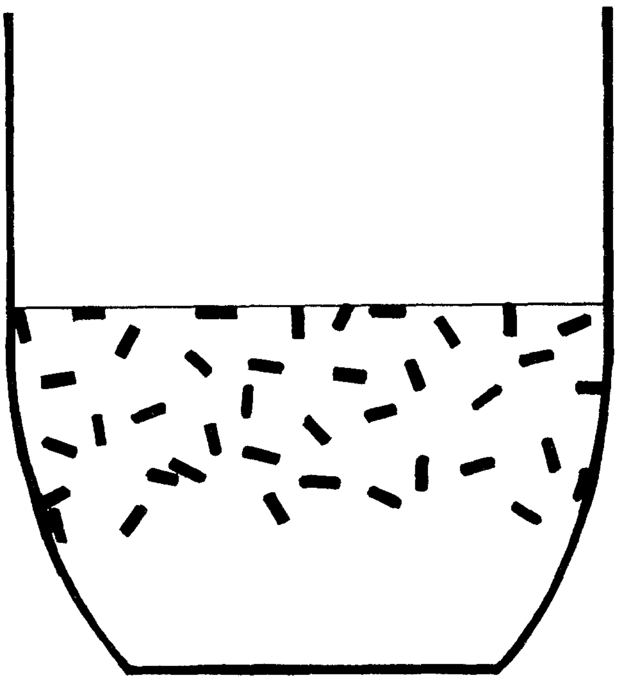

Figure 4 A schematic drawing to show the mode of occurrence of emerald crystals in high-temperature solution.

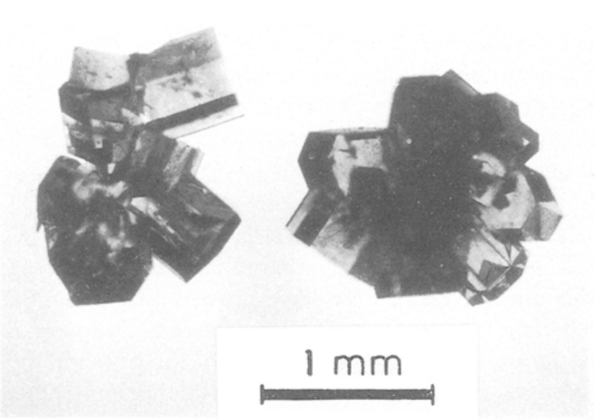

Figure 5 Transmission optical micrograph showing aggregates of emerald crystals.

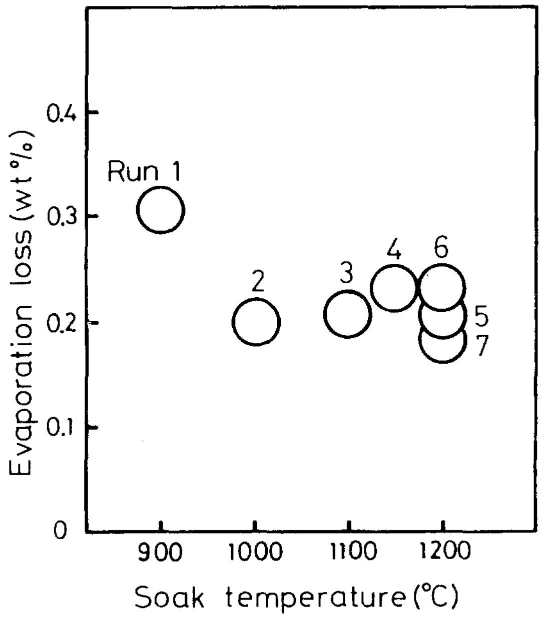

Figure 6 Variation of evaporation loss of flux with soak temperature.

range 0.18 (about 0.06 g)–0.31 wt% (about 0.10 g) were observed. The volatility values were very small, and were almost independent of the soak temperature or the composition of the mixtures. It is found that the $PbO \cdot V_2O_5$ flux is not very volatile at high temperatures. While a disadvantage of the PbO flux alone is its high volatility, the addition of V_2O_5 to PbO greatly reduces the degree of volatility. In these growth runs, the influence of evaporation on the nucleation and crystal growth of emerald was negligible. The low volatility permits the use of the $PbO \cdot V_2O_5$ flux at temperatures higher than those normally used. As a result prolonged growth experiments may be conducted. Another disadvantage of PbO alone is its toxicity. Poisonous vapours from the hot furnace are dangerous and may cause illnesses. From the standpoint of the health of flux-growers, a low volatility of the $PbO \cdot V_2O_5$ flux is desirable. The $PbO \cdot V_2O_5$ flux has the advantage of very low volatility.

The platinum crucibles were found to be undamaged after use in these growth runs: the $PbO \cdot V_2O_5$ flux did not attack the platinum crucibles, and thus is compatible with platinum over the intended temperature range. It has been reported that V_2O_5 protects the platinum crucibles by oxidizing traces of free lead [5]. While PbO alone attacks platinum crucibles severely, the addition of V_2O_5 to PbO reduces the attack on platinum and lengthens the life of the crucibles.

In addition, the $PbO \cdot V_2O_5$ flux used for the growth of emerald crystals had the following advantages: (1) low melting point, (2) ready availability in high purity at reasonable cost, (3) ease of separation from grown crystals by chemical means, and (4) ease of preparation by mixing the components.

It was found that the $PbO \cdot V_2O_5$ flux was a suitable flux to grow emerald crystals.

3.3. Characteristics of the emerald crystals obtained

The emerald crystals obtained were the typical emerald-green colour. They were up to 1.8 mm in size and transparent. The crystals were hexagonal-rod shaped, and the crystals surfaces were very flat. In order to determine the Miller indices of the grown crystal faces, the crystals were laid on a holder plate and investigated by the XRD. Fig. 7 shows XRD

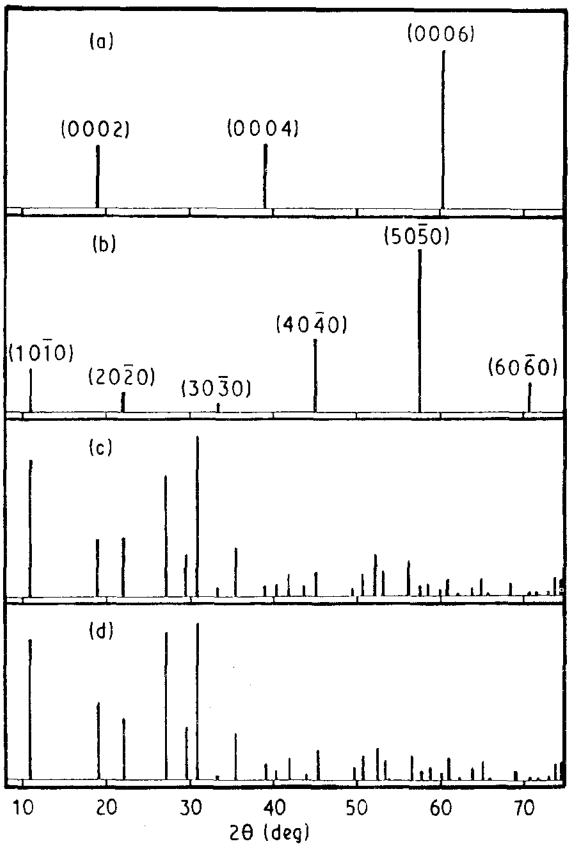

Figure 7 X-ray diffraction patterns (CuK_α) of emerald crystals. (a) Hexagonal crystal of which base was laid in parallel with the holder plate; (b) hexagonal crystal of which the prism was laid in parallel with the holder plate; (c) pulverized crystallite; (d) beryl (emerald) JCPDS data [10].

profiles of hexagonal rod crystals, pulverized crystallites and beryl (emerald) JCPDS data [10]. As shown in Fig. 7a and b, only the diffraction patterns of the $(000l)$ and $(h0i0)$ planes were predominant, respectively. The X-ray data of emerald crystals shows a combination of the base (0001) and prism $(10\bar{1}0)$. The hexagonal rod crystals are bounded by the well-developed $\{0001\}$ and $\{10\bar{1}0\}$ faces. The form of emerald crystals is a regular hexagonal rod, and the habit is independent of growth conditions in Runs 2–7.

Figure 8 Transmission optical micrograph showing flux inclusions in the emerald crystals grown.

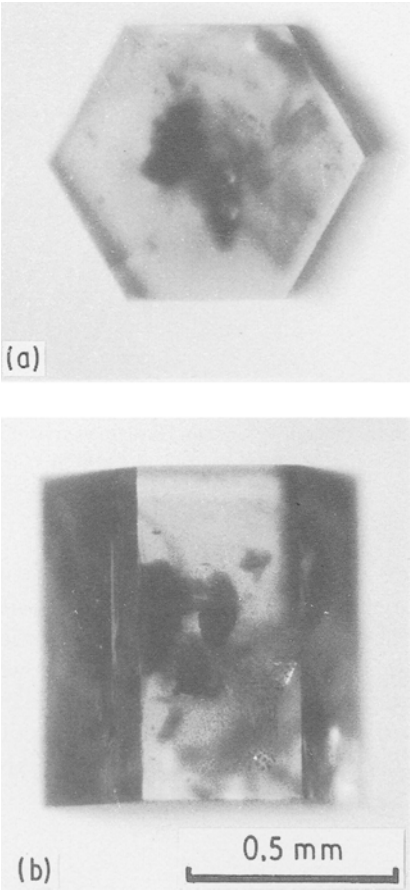

Figure 9 Higher magnification transmission optical micrographs showing flux inclusions in an emerald crystal viewed (a) from above and (b) from the side.

The emerald crystals showed various kinds of imperfections, and even good crystals were also present. Fig. 8 shows the inclusions observed by the use of the microscope in emerald crystals. A higher magnification micrograph of inclusions in an emerald crystal is shown in Fig. 9. Inclusions were located within the well-formed transparent crystals. It is considered that flux was trapped by the growing crystal when they were in the high-temperature solution. This is evidence of an internal defect in a crystal suggesting that some considerable degree of supersaturation is first experienced and a rapid growth stage follows nucleation. The flux inclusions were thus formed and subsequently higher-quality growth occurs on the outer surfaces at a slower rate.

Opaque dark-green crystals were also present, up to about 5% in number of the total crystals obtained in Runs 2–5. The higher the soak temperature, the smaller was the number of opaque dark-green crystals grown. They rarely grew in Runs 6 and 7. Typical opaque dark-green crystals are shown in Fig. 10. The surfaces of the crystals were not smooth: hexagonal branches of small emerald crystals nucleated and grew at the surface of the large crystals previously grown. It is suggested that local variations in supersaturation

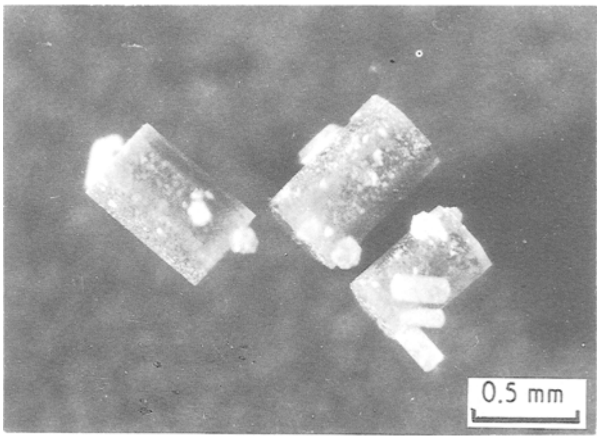

Figure 10 Reflection optical micrograph showing opaque dark-green crystals of emerald.

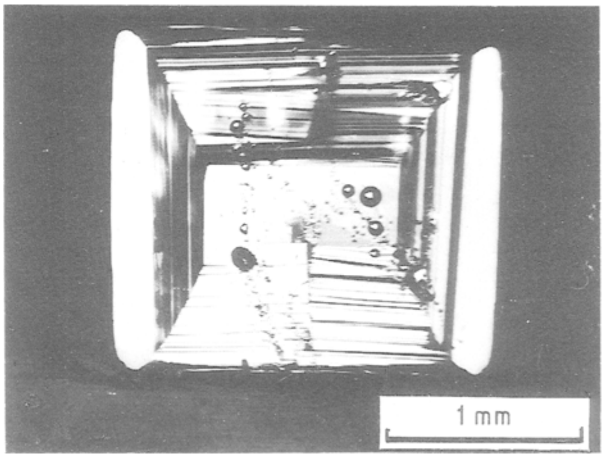

Figure 11 Reflection optical micrograph showing hopper-shaped emerald growing at the surface of a high-temperature solution of $PbO \cdot V_2O_5$ flux. The black parts correspond to solidified solution.

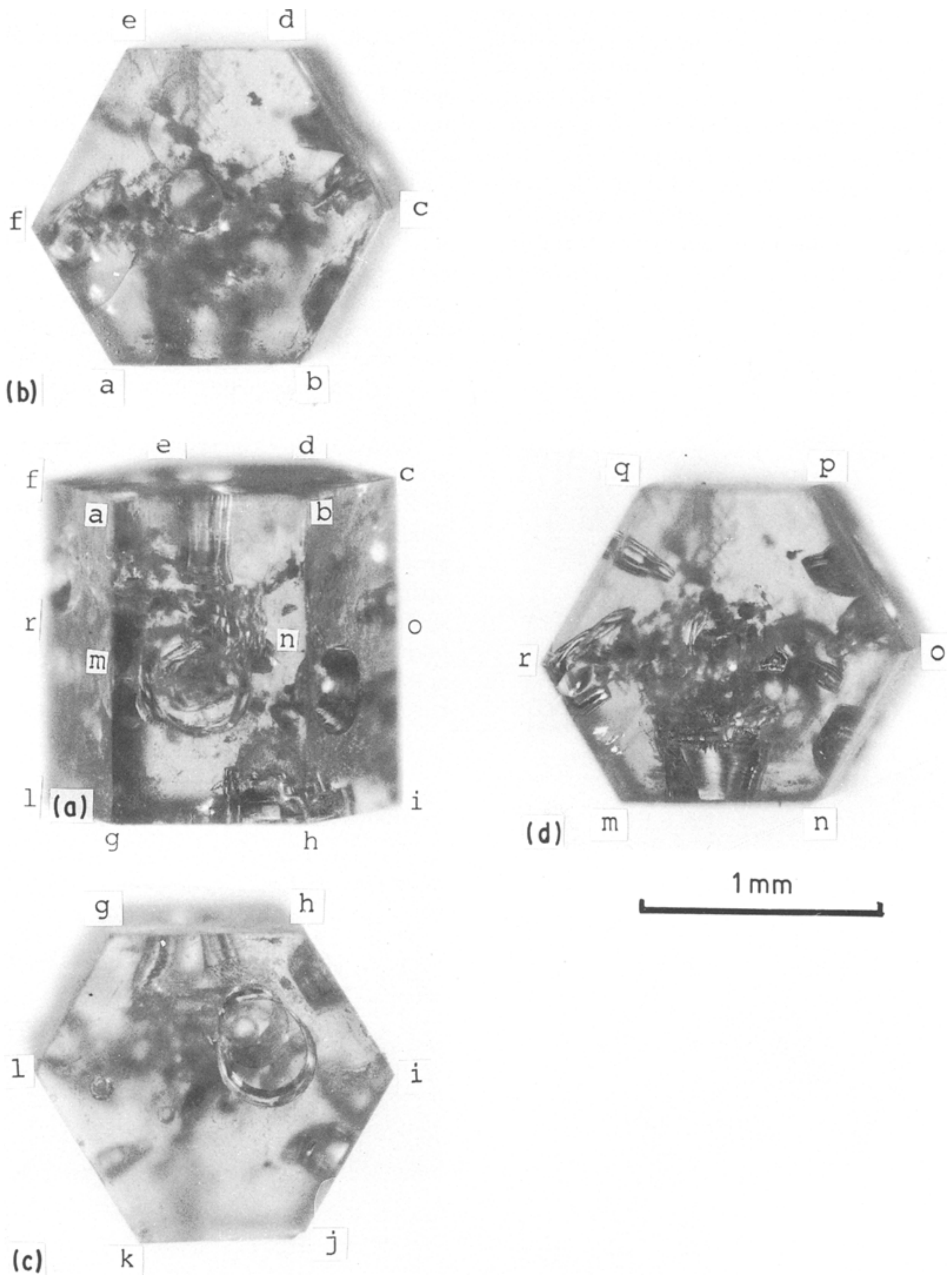

Figure 12 Transmission optical micrograph showing cylinder-shaped cavities within the emerald crystal. (a) Hexagonal crystal with cavities; (b, c) the same crystal viewed from (b) above and (c) below; (d) the same crystal viewed from above in focus at about m–r.

were present in the high-temperature solution and opaque emerald crystals grew in those parts with a high degree of supersaturation.

Hopper crystals of emerald were often formed at the surface of the high-temperature solution. Fig. 11 shows a hopper face on an emerald crystal grown in the $PbO \cdot V_2O_5$ flux. Growth across the hopper face is prevented in crystals floating at the surface of the solution, because the upper face is not in contact with the solution. Growth continues on the sides of the floating hopper.

Cylinder-shaped cavities were also observed on the $\{0001\}$ and $\{10\bar{1}0\}$ faces of emerald crystals. The cavities, shown in Fig. 12, were up to 0.45 mm diameter and up to 0.35 mm deep. They seem to have formed as a result of the limit in diffusion of solute ions or the local variation in supersaturation.

Hexagonal rod crystals of emerald, which were green and transparent, grew under stable conditions. On the other hand, most of the imperfections in the emerald crystals grown result from a too rapid growth under unstable conditions.

4. Conclusions

1. Emerald crystals were grown by slow cooling in the $PbO \cdot V_2O_5$ flux.
2. The emerald crystals were up to 1.8 mm in size,

green and transparent. Their form was a regular hexagonal rod bounded by the $\{0001\}$ and $\{10\bar{1}0\}$ faces.

3. About 9.0 g emerald was dissolved in 100 g $PbO \cdot V_2O_5$ at 1200 °C. The solubility decreased gradually with decreasing temperature.

4. On the basis of the solubility data, the presence of undissolved particles in the solution was found to be a necessary condition for the growth of large emerald crystals.

5. Unsaturated solution at the soak temperature produced good and relatively small emerald crystals in a subsequent slow cooling experiment.

6. Advantages of the $PbO \cdot V_2O_5$ flux are also mentioned.

7. Various kinds of imperfections in the emerald crystals grown were observed.

References

1. P. HAUTEFEUILLE and A. PERREY, *Compt. Rend.* **106** (1888) 1800.
2. D. ELWELL, "Man-Made Gemstones" (Ellis Horwood, Chichester, 1979) pp. 27, 58.
3. R. P. MILLER and R. A. MERCER, *Mineral. Mag.* **35** (1965) 250.
4. D. ELWELL and H. J. SCHEEL, "Crystal Growth from High-Temperature Solutions" (Academic Press, London, 1975) pp. 34, 564, 616.
5. B. M. WANKLYN, *J. Crystal Growth* **7** (1970) 368.
6. G. GARTON, S. H. SMITH and B. M. WANKLYN, *ibid.* **13/14** (1972) 588.
7. E. M. LEVIN, C. R. ROBBINS and H. F. McMURDIE, "Phase Diagrams for Ceramists" (The American Ceramic Society, Columbus, 1964) p. 117.
8. R. C. LINARES, *Amer. Mineral.* **52** (1967) 1554.
9. M. USHIO and Y. SUMIYOSHI, *Nippon Kagaku Kaishi* (1972) 1648.
10. JCPDS 9-430.
11. J. P. REMEIKA, *J. Amer. Chem. Soc.* **76** (1954) 940.
12. R. C. DeVRIES and G. W. SEARS, *J. Chem. Phys.* **34** (1961) 616.
13. B. M. WANKLYN and H. A. LIPKO, *J. Crystal Growth* **49** (1980) 182.
14. S. OISHI and M. HIRAO, *Bull. Chem. Soc. Jpn* **63** (1990) 984.
15. R. A. LEFEVER, A. B. CHASE and L. E. SOBON, *Amer. Mineral.* **47** (1962) 1450.
16. H. KOJIMA, *Seramikkusu* **3** (1968) 497.
17. S. ASHIDA, *Kobutsugaku Zasshi* **8** (1968) 407.
18. M. INOUE, T. MORISHITA, E. NARITA and T. OKABE, *Nippon Kagaku Kaishi* (1979) 1489.

Received 9 July 1990
and accepted 6 February 1991